Translational Oncology 14 (2021) 101019

Contents lists available at ScienceDirect

Translational Oncology

journal homepage: www.elsevier.com/locate/tranon

Original Research

Minimal residual disease in high-risk neuroblastoma shows a dynamic and disease burden-dependent correlation between bone marrow and peripheral blood

Kyaw San Lin[a], Suguru Uemura[a], Khin Kyae Mon Thwin[a], Naoko Nakatani[a], Toshiaki Ishida[b], Nobuyuki Yamamoto[a], Akihiro Tamura[b], Atsuro Saito[b], Takeshi Mori[b], Daiichiro Hasegawa[b], Yoshiyuki Kosaka[b], Nanako Nino[a], China Nagano[a], Satoru Takafuji[a], Kazumoto Iijima[a], Noriyuki Nishimura[c,*]

[a] Department of Pediatrics, Kobe University Graduate School of Medicine, Kobe, Japan
[b] Department of Hematology and Oncology, Kobe Children's Hospital, Kobe, Japan
[c] Department of Public Health, Kobe University Graduate School of Health Science, Kobe, Japan

ARTICLE INFO

Keywords:
Neuroblastoma (NB)
Minimal Residual Disease (MRD)
Peripheral Blood (PB)
Circulating Tumor Cell (CTC)
Bone Marrow (BM)
Disseminated Tumor Cell (DTC)

ABSTRACT

Neuroblastoma (NB) is the most common extracranial solid tumor in children and originates from sympathoadrenal or Schwann cell precursors derived from neural crest. These neural crest derivatives also constitute the hematopoietic and mesenchymal stem cells in bone marrow (BM) that is the most frequent site of NB metastasis and relapse. In NB patients, NB cells have been pathologically detected in BM and peripheral blood (PB), and minimal residual disease (MRD) in BM and PB (BM-MRD and PB-MRD) can be monitored by quantitating several sets of NB-associated mRNAs (NB-mRNAs). Although previous studies have shown varying degrees of correlation between BM-MRD and PB-MRD, the underlying factors and/or mechanisms remains unknown. In the present study, we determined the levels of BM-MRD and PB-MRD by quantitating seven NB-mRNAs in 133 pairs of concurrently collected BM and PB samples from 19 high-risk NB patients with clinical disease evaluation, and examined their correlation in overall and subgroups of sample pairs. The levels of BM-MRD and PB-MRD were moderately ($r = 0.418$, $p < 0.001$) correlated with each other in overall sample pairs. The correlation became strong ($r = 0.725$, $p < 0.001$), weak ($r = 0.284$, $p = 0.008$), and insignificant ($p = 0.194$) in progression, stable, and remission subgroups of sample pairs, respectively. It also became stronger in subgroups of sample pairs with poor treatment responses and poor prognostic factors. Present study suggests that MRD in high-risk NB shows a dynamic and disease burden-dependent correlation between BM and PB.

Introduction

Neuroblastoma (NB) is the most common extracranial solid tumor in children and originates from sympathoadrenal precursors (SAPs) or Schwann cell precursors (SCPs) that constitute major derivatives of neural crest (NC) [1–3]. Patients with high-risk NB account for approximately half of newly diagnosed cases and their long-term survival rate remains around 40–50%. Despite extensive multimodal treatment, more than half of high-risk patients experience tumor relapse/regrowth due to chemoresistant minimal residual disease (MRD). Patients with relapsed/regrown NB were rarely cured with less than 10% of long-term survival [4–6]. To achieve optimal outcome for high-risk NB patients, the accurate MRD detection is essential to monitor the disease burden and treatment response. Since no recurrent oncogenic-fusion gene is identified in NB cells, MRD have been identified by detecting neuroblastoma-associated mRNAs (NB-mRNAs) with quantitative PCR (qPCR) [7,8]. Several sets of NB-mRNAs were shown to possess a significant prognostic value for NB patients [9–12]. However, these sets adopted considerably different NB-mRNAs and had significant but limited prognostic information (0.5 < area under curve (AUC) < 0.7: low accuracy) [12]. We have recently developed a new MRD assay that quantified 7NB-mRNAs (CRMP1, DBH, DDC, GAP43, ISL1, PHOX2B, and TH mRNAs) by droplet digital PCR (ddPCR) and demonstrated that this ddPCR-based MRD assay outperformed the qPCR-based MRD assay and possessed significant and better prognostic information (0.7 < AUC < 0.9: moderate accuracy) [13].

MRD is defined as residual cancer cells that persistently reside in patients following local and systemic therapies [14]. It persists as cancer

* Corresponding author.
E-mail address: nnishi@med.kobe-u.ac.jp (N. Nishimura).

https://doi.org/10.1016/j.tranon.2021.101019
Received 31 August 2020; Received in revised form 20 October 2020; Accepted 12 January 2021

stem cells (CSCs) in primary tumor, circulating tumor cells (CTCs) in peripheral blood (PB), and disseminated tumor cells (DTCs) in bone marrow (BM), lymph node, and micrometastasis in other tissues [15, 16]. In many cancer types, MRD evaluation is clinically performed by detecting CTC in PB and/or DTC in BM due to the invasive nature of surgical biopsies for CSC in primary tumor [17]. In hematologic malignancies that originate from the hematopoietic stem cells with distinct differentiation stages, CTC in PB is directly derived from DTC and/or CSC resided in the same BM. Accordingly, MRD can be evaluated in PB as well as BM in acute lymphoblastic leukemia (ALL) [18], acute myeloid leukemia (AML) [19], and chronic myelogenous leukemia (CML) [20]. In non-hematopoietic solid tumors, MRD detection in PB depends on cancer types [21–23].

In the case of NB, the origin of NB (SCP-containing NC derivatives) is shown to migrate and constitute hematopoietic and mesenchymal stem cells in BM by mouse genetic models [3,24–27]. In human NB patients, BM is known to be the most frequent site of metastasis and relapse [28]. NB cells are pathologically detected in PB at diagnosis and during therapy [29,30], and high expression of two sets of NB-mRNAs in PB at diagnosis were associated with poor outcome [10,31]. Although the distinct sets of NB-mRNAs for detecting BM-MRD and PB-MRD and the differential NB-mRNAs expression in BM and PB samples were reported in the past [32,33], the more recent studies revealed the significantly correlated expression of 5NB-mRNAs between BM and PB by qPCR [12]. We have also found that the expression of 7NB-mRNAs was significantly correlated between BM and PB but was approximately 100 times higher in BM than PB in 60 pairs of BM and PB samples from 16 high-risk NB patients by ddPCR [13].

Although previous studies have shown varying degrees of correlation between BM-MRD and PB-MRD, the underlying factors and/or mechanisms remains unknown. In mouse genetic models, NB has shown to originate from SCPs, which consist of NC derivatives and can migrate into the BM. However, the precise origin (which cells of NC derivatives) of NB, a disease metastasized primarily to the BM, has not clarified yet in human samples. To reveal the underlying factors and/or mechanisms, an example of human BM and PB samples consistent or inconsistent with mouse genetic models would provide an important foundation. In the present study, we determined the levels of BM-MRD and PB-MRD by quantitating 7NB-mRNAs in 133 pairs of concurrently collected BM and PB samples from 19 high-risk NB patients with clinical disease evaluation, and examined their correlation in overall and subgroups of sample pairs.

Materials and methods

NB patients and samples

All NB patients were diagnosed and stratified into high-risk according to the Children' s Oncology Group (COG) Neuroblastoma Risk Stratification System [5,34] or the International Neuroblastoma Risk Group (INRG) Classification System [35,36], and treated at Kobe Children Hospital or Kobe University Hospital between November 2011 and August 2019 based on the JN-H-11 (UMIN000005045) [37] or JN-H-15 (UMIN000016848) protocol of the Japanese Children's Cancer Group (JCCG) Neuroblastoma Committee (JNBSG). All BM and PB samples with written informed consent were concurrently (less than 3 days apart) collected as frequently as possible during the entire course of treatment. This study was approved by the ethics committee at Kobe University Graduate School of Medicine (No.180278) and Kobe Children's Hospital (No.30–80) and was conducted following the guidelines for Clinical Research of Kobe University Graduate School of Medicine.

Disease evaluation

Disease evaluation was conducted as described previously [13]. Briefly, evaluation was conducted at every collection time point in accordance with the INRC based on the available medical records [28,38]. Responses were assigned to "remission" corresponding to complete response (CR) or very good partial response (VGPR), "stable" corresponding to partial response (PR), mixed response (MR), or no response (NR), or "progression" corresponding to progressive disease (PD) for all BM and PB sample pairs.

Sample preparation and 7NB-mRNAs ddPCR assay

Sample preparation and 7NB-mRNAs ddPCR assay were performed as described previously [13]. Briefly, all BM and PB samples were separated using Mono-Poly resolving medium (DS Pharma Biomedical, Osaka, Japan), and nucleated cells were collected. Total RNA was extracted with a TRIzol Plus RNA purification kit (Life Technologies, Carlsbad, CA). cDNA was synthesized from 1 or 0.5 μg total RNA using a Quantitect reverse transcription kit (Qiagen, Valencia, CA, USA) and stored at −80 °C until use. 7NB-mRNAs ddPCR assay measured the expression of 7 NB-mRNAs (CRMP1, DBH, DDC, GAP43, ISL1, PHOX2B, and TH) and a reference gene mRNA (HPRT1) with optimized probe and primer sets, cDNA, and standard thermal cycling conditions using a QX200 ddPCR system (Bio-Rad Laboratories, Hercules, CA) according to the digital MIQE (Minimum Information for Publication of Quantitative Digital PCR Experiments) guideline [39]. The level of 7NB-mRNAs (combined signature) was defined as the weighted sum of 7 relative copy numbers (level of each NB-mRNA), in which the reciprocal of 90 percentile in non-NB control samples was used for the weighting for each NB-mRNA. For BM samples, the level of 7NB-mRNAs was calculated as the mean of right and left samples.

Statistical analysis

Correlation of the level of 7NB-mRNAs between BM and PB samples was assessed by Spearman's rank correlation test. Reported P values were two-sided and $p < 0.05$ was considered statistically significant. Correlation coefficient r values were considered 0.00–0.09 as "negligible", 0.10–0.39 as "weak", 0.40–0.69 as "moderate", 0.70–0.89 as "strong", and 0.90–1.00 as "very strong" according to the previous report [40]. AUC was interpreted 0.50–0.69 as "low accuracy", 0.70–0.89 as "moderate accuracy", and 0.90–1.00 as "high accuracy" according to the previous report [41]. EZR (version 1.35, www.jichi.ac.jp/saitama-sct/SaitamaHP.files/statmedEN.html; Saitama Medical Center, Jichi Medical University, Saitama, Japan), which is a modified version of R commander designed to add statistical functions frequently used in biostatistics [42] was used for statistical analyses.

Results

Patient and sample characteristics

To investigate the underlying factors and/or mechanisms for varying degrees of correlation between BM-MRD and PB-MRD [12,13], we have extended our cohort of NB patients and samples to cover the entire course of high-risk NB treatment [13,33,43]. In addition to 60 sample pairs from 16 high-risk NB patients previously analyzed [13], we have newly analyzed 73 sample pairs from 19 high-risk NB patients in the present study. As summarized in Table 1, a total of 19 high-risk NB patients were analyzed and they showed the typical characteristics of high-risk NB: 84% (16/19) were ≧18 months old, 74% (14/19) with adrenal grand tumor, 84% (16/19) with BM metastasis at diagnosis, 100% (19/19) with unfavorable tumor, 74% (13/17) with diploid tumor, 37% (7/19) with MYCN-amplified tumor, 58% (11/19) with relapse/regrowth, and 36% (4/11) with BM-relapse/regrowth (Table 1). From these high-risk NB patients, a total of 133 pairs of BM and PB samples were concurrently (less than 3 days apart) collected as frequently as possible during the entire course of treatment.

Table 1
Patient characteristics.

Variable	Category	Patients (%)
Sex	Male	13 (68%)
	Female	6 (32%)
Age at diagnosis	<18 months	3 (16%)
	≧18 months	16 (84%)
Primary tumor site	Adrenal gland	14 (74%)
	Non-adrenal gland	5 (26%)
BM metastasis at diagnosis	Present	16 (84%)
	Absent	3 (16%)
Histopathology	Favorable	0 (0%)
	Unfavorable	19 (100%)
DNA ploidy	Diploid	14 (74%)
	Hyperdiploid	3 (16%)
MYCN status	Amplified	7 (37%)
	Non-amplified	12 (63%)
Relapse/regrowth	Present	11 (58%)
	Absent	8 (42%)
Recurrent tumor site	BM	4 (36%)
	Non-BM	7 (64%)

BM, bone marrow; MYCN, MYCN proto-oncogene, bHLH transcription factor.

Table 2
Sample characteristics.

Attribute	Variable	Category	Samples (%)
Sample	BM infiltration at sampling	Present	21 (16%)
		Absent	112 (84%)
	Collection time point	Diagnosis	10 (7%)
		Treatment	32 (24%)
		Post-treatment	36 (27%)
		Relapse	9 (7%)
		Post-relapse	46 (35%)
	Disease status	Remission	21 (16%)
		Stable	87 (65%)
		Progression	25 (19%)
Patient	Sex	Male	87 (65%)
		Female	46 (35%)
	Age at diagnosis	<18 months	26 (20%)
		≧18 months	107 (80%)
	Primary tumor site	Adrenal gland	106 (80%)
		Non-adrenal gland	27 (20%)
	BM metastasis at diagnosis	Present	122 (92%)
		Absent	11 (8%)
	Histopathology	Favorable	0 (0%)
		Unfavorable	133 (100%)
	DNA ploidy	Diploid	93 (70%)
		Hyperdiploid	33 (25%)
	MYCN status	Amplified	45 (34%)
		Non-amplified	88 (66%)
	Relapse/regrowth	Present	90 (68%)
		Absent	43 (32%)
	Recurrent tumor site	BM	32 (36%)
		Non-BM	58 (64%)

BM, bone marrow; MYCN, MYCN proto-oncogene, bHLH transcription factor.

As shown in Table 2, a total of 133 sample pairs were analyzed and they were subdivided into subgroups according to each sample or patient evaluation. For each sample evaluation, all BM samples were pathologically analyzed by histology/immunohistochemistry (IHC) of biopsies or cytology/immunocytology (IC) of aspirates according to the International Neuroblastoma Response Criteria (INRC) recommendations [28], resulting in 21 BM infiltration at sampling-positive samples among 133 samples. Sample collection time points were defined as “diagnosis” at initial diagnosis, “treatment” including induction chemotherapy, high-dose chemotherapy with autologous peripheral blood stem cell transplantation (PBSCT), surgery, and radiation, “post-treatment” including 13-cis-retinoic acid (13-cis-RA) treatment and follow-up before relapse, “relapse” at relapse diagnosis, and “post-relapse” including all treatment and follow-up after relapse, resulting in

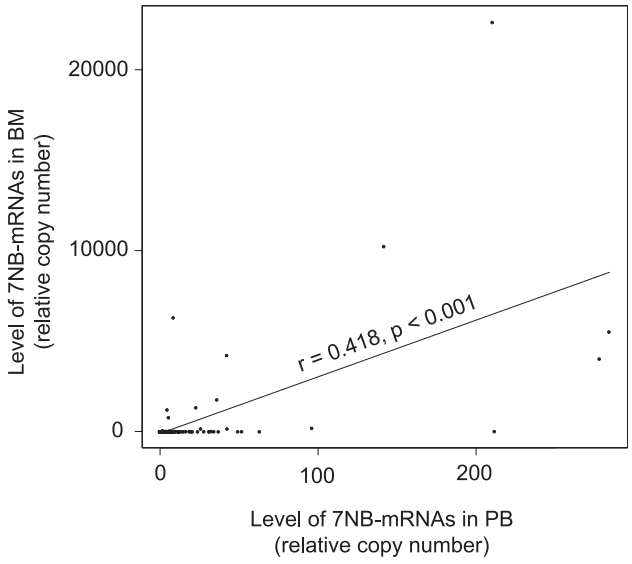

Fig. 1. Correlation of the levels of 7 neuroblastoma-associated mRNAs (7NB-mRNAs) between bone marrow (BM) and peripheral blood (PB) in overall sample pairs. The level of 7NB-mRNAs (relative copy number) in 133 overall sample pairs of concurrently collected BM and PB samples was determined by droplet digital PCR (ddPCR).

10 diagnosis, 32 treatment, 36 post-treatment, 9 relapse, and 46 post-relapse samples. Disease status at sampling were retrospectively evaluated as remission, stable, and progression, resulting in 21 remission, 87 stable, and 25 progression samples (Table 2). For each patient evaluation, samples were stratified by the following prognostic factors: 80% (107/133) were derived from ≧18 months old patients, 80% (106/133) from patients with adrenal grand tumor, 92% (122/133) from patients with BM metastasis at diagnosis, 70% (93/126) from patients with diploid tumor, 34% (45/133) from patients with MYCN-amplified tumor, 68% (90/133) from relapsed/regrown patients, and 36% (32/90) from BM-relapsed/regrown patients (Table 2).

Correlation between BM-MRD and PB-MRD in overall sample pairs

We first determined the levels of BM-MRD and PB-MRD by quantitating 7NB-mRNAs and analyzed their correlation in 133 overall sample pairs. BM-MRD showed a moderate correlation with PB-MRD ($r = 0.418$, $p < 0.001$). However, the level of BM-MRD was approximately 10–100 times higher than that of PB-MRD (Fig. 1). Although this was consistent with previous studies [12,13], the difference in the degree of correlation between BM-MRD and PB-MRD was further increased in the present overall sample pairs.

Correlation between BM-MRD and PB-MRD in subgroups according to each sample evaluation

We then performed a subgroup analysis according to each sample evaluation; BM infiltration at sampling, disease status, and collection time point (Table 2). In subgroups according to BM infiltration at sampling, the correlation between BM-MRD and PB-MRD was strong ($r = 0.736$, $p < 0.001$) and weak ($r = 0.306$, $p = 0.001$) in the positive and negative subgroup, respectively (Fig. 2A). In subgroups according to disease status, it became stronger with disease progression; a strong correlation ($r = 0.725$, $p < 0.001$) in the progression subgroup, a weak correlation ($r = 0.284$, $p = 0.008$) in the stable subgroup, and an insignificant correlation ($p = 0.295$) in the remission subgroup (Fig. 2B). In subgroups according to collection time point, strong ($r = 0.7$, $p = 0.043$) and moderate ($r = 0.615$, $p < 0.001$) correlations were found in the relapse

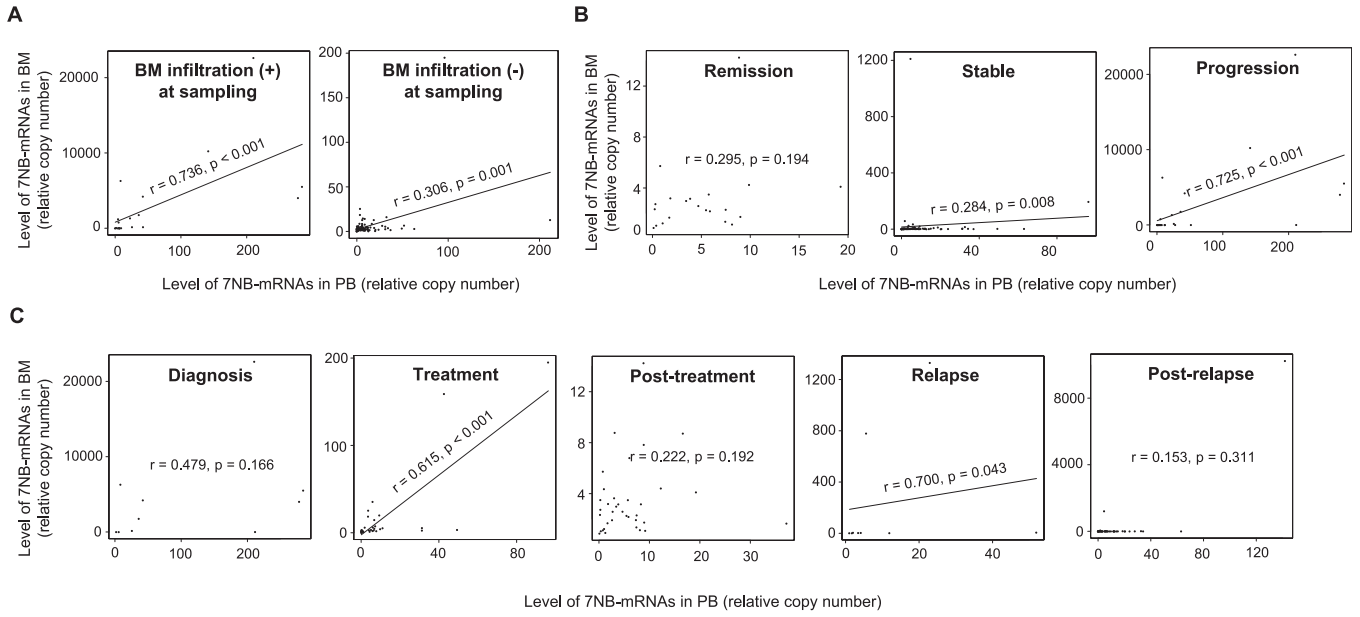

Fig. 2. Correlation of the levels of 7 neuroblastoma-associated mRNAs (7NB-mRNAs) between bone marrow (BM) and peripheral blood (PB) in subgroups according to each sample evaluation. The level of 7NB-mRNAs (relative copy number) in concurrently collected BM and PB samples was determined by droplet digital PCR (ddPCR) in subgroups according to BM infiltration at sampling (A), disease status (B), and collection time point (C). (A) BM infiltration (+) 21 sample pairs, BM infiltration (-) 112 sample pairs. (B) remission 21 sample pairs, sTable 87 sample pairs, and progression 25 sample pairs. (C) diagnosis 10 sample pairs, treatment 32 sample pairs, post-treatment 36 sample pairs, relapse 9 sample pairs, and post-relapse 46 sample pairs.

and treatment subgroups, respectively. There was no significant correlation ($p = 0.166$–0.311) in the diagnosis, post-treatment, and post-relapse subgroups (Fig. 2C).

Correlation between BM-MRD and PB-MRD in subgroups according to each patient evaluation

Next, we analyzed the correlation between BM-MRD and PB-MRD in subgroups according to each patient evaluation; age at diagnosis, primary tumor site, BM metastasis at diagnosis, DNA ploidy, MYCN status, relapse/regrowth, and recurrent tumor site (Table 2). Among these evaluations, age at diagnosis, BM metastasis at diagnosis, and DNA ploidy had a strong impact on the correlation between BM-MRD and PB-MRD (Fig. 3, Supplementary Figure 1). In subgroups of ≧18 months at diagnosis, BM metastasis present at diagnosis, and diploid tumor, moderate correlations ($r = 0.418$–478, $p < 0.001$) were detected. In contrast, no statistically significant correlation ($p = 0.080$–0.438) was found in subgroups of <18 months at diagnosis, BM metastasis absent at diagnosis, and hyperdiploid tumor (Fig. 3).

Discussion

In the present study, we determined the levels of BM-MRD and PB-MRD by quantitating 7NB-mRNAs in 133 pairs of concurrently collected BM and PB samples from 19 high-risk NB patients with clinical disease evaluation, and revealed a dynamic and disease burden-dependent correlation of MRD between BM and PB. To our knowledge, this is the first study to demonstrate that the correlation between BM-MRD and PB-MRD is associated with the disease burden in non-hematopoietic solid tumors.

Over the past decades, the sensitivity of MRD detection has been improved with the introduction of new techniques [16]. Conventional pathology (histology/IHC) is not always possible to detect the tumor cells below the level of 10^{-2}. The sensitivity of cytology/IC and flow cytometry (FCM) depends on the number of investigated cells and reaches below the level of 10^{-3}–10^{-4}. qPCR and ddPCR are able to detect tumor cells below the level of 10^{-4}–10^{-6}. Accordingly, the NB patients with BM-metastasized/infiltrated tumor cells in the level of 10^{-4}–10^{-6} are evaluated as remission (no evidence of disease evaluated by histology/IHC or cytology/IC) but are positive for BM-MRD detected by ddPCR. In the present study, BM-MRD and PB-MRD (the level of 7NB-mRNAs) are detected and determined by ddPCR in all 133 BM and PB samples (0.1–22,630.8 copies for BM-MRD; 0.1–284.5 copies for PB-MRD), and 112 out of 133 BM samples are negative for BM-infiltration but positive for BM-MRD as described before [13].

Although NB cells and MRD had been detected in PB since early 1990 [10,29–31], there were superficially conflicting studies about the relation of NB-mRNAs expression between BM and PB [12,13,32,33]. The older two studies did not directly analyze the levels of NB-mRNAs between BM and PB, but indirectly compared their orders and reported the distinct NB-mRNAs sets for BM-MRD and PB-MRD and the differential NB-mRNAs expression in BM and PB samples, respectively [32,33]. Actually, they were not inconsistent with the newer two studies reporting a significant correlation between BM-MRD and PB-MRD [12,13]. However, the degree of correlation was considerably varied in these different cohorts of NB patients and samples. In the present study, we tried to increase the number of patients and samples as much as possible to identify a particular subgroup of patients or samples having strong or no correlation, and collected a total of 133 sample pairs covering the entire course of high-risk NB treatment (10 diagnosis, 32 treatment, 36 post-treatment, 9 relapse, and 46 post-relapse sample pairs), all disease status (21 remission, 87 stable, and 25 progression sample pairs), and 12 patients with comparable number of sample pairs (> 6 sample pairs per patient). Overall and subgroup analysis of the present sample pairs had successfully revealed a dynamic and disease burden-dependent correlation between BM-MRD and PB-MRD. The present study clearly explain the different r values between the subgroup of relapsed/progressive or refractory high-risk NB patients ($r = 0.670$) [12] and the overall high-risk NB patients ($r = 0.613$) [13], and also between our previous cohort ($r = 0.613$, in 23% remission, 49% stable, and 28% progression samples) [13] and present cohort ($r = 0.418$,16% remission, 65% stable, and 19% progression samples) (Fig. 1 and Table 2).

The most striking results of the present study was obtained from the subgroup analysis according to disease status of each sample. Dis-

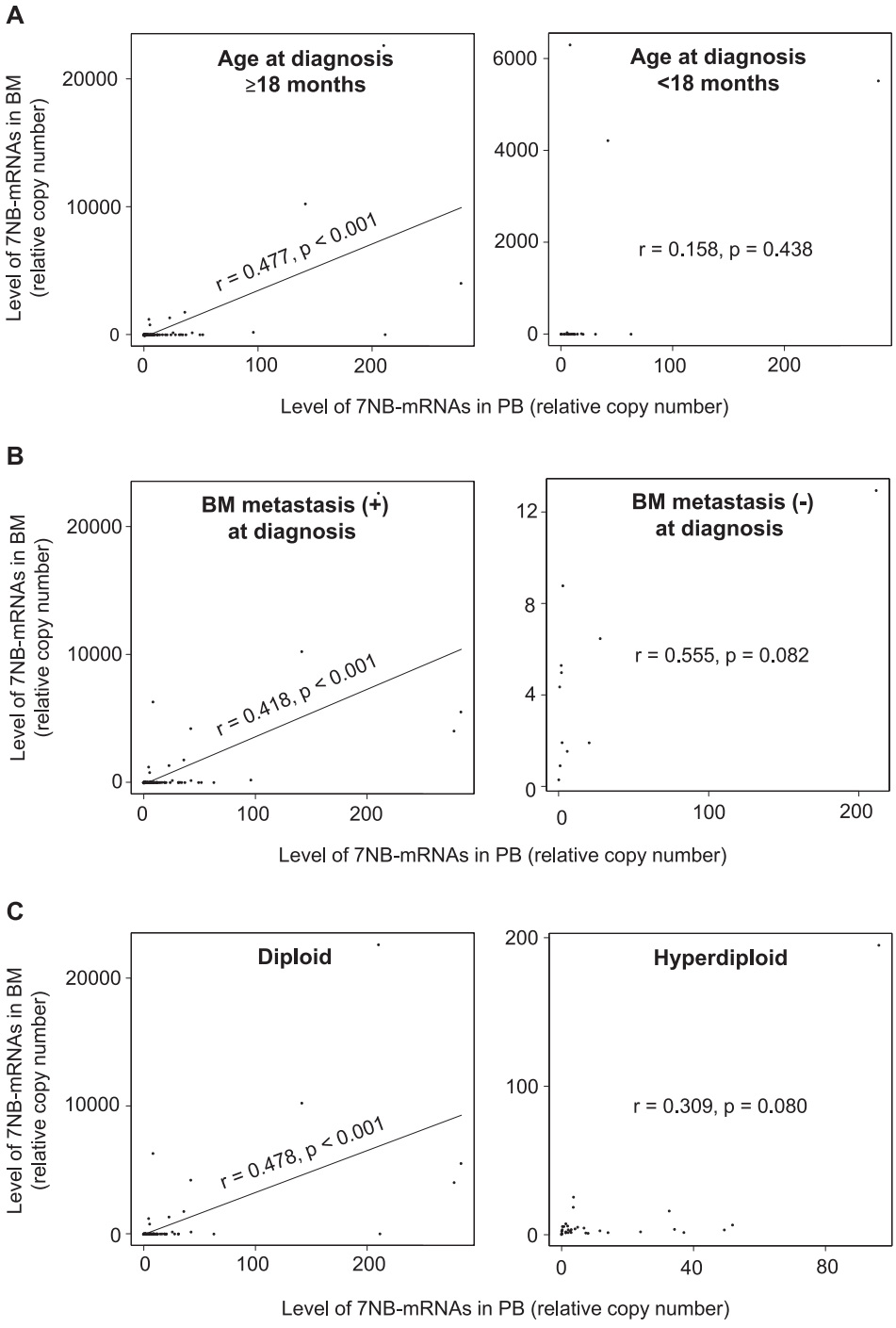

Fig. 3. Correlation of the levels of 7 neuroblastoma-associated mRNAs (7NB-mRNAs) between bone marrow (BM) and peripheral blood (PB) in subgroups according to each patient evaluation. The level of 7NB-mRNAs (relative copy number) in concurrently collected BM and PB samples was determined by droplet digital PCR (ddPCR) in subgroups according to age at diagnosis (A), BM metastasis at diagnosis (B), and DNA ploidy (C). (A) ≧18 months 107 sample pairs, <18 months 26 sample pairs. (B) BM metastasis (+) 122 sample pairs, BM metastasis (-) 11 sample pairs. (C) diploid 93 sample pairs, hyperdiploid 33 sample pairs.

ease status was found to stratify 133 sample pairs into the strongly correlated-progression subgroup of 25 sample pairs (r = 0.725), the weakly correlated-stable subgroup of 87 sample pairs (r = 0.284), and the uncorrelated-remission subgroup of 21 sample pairs (Fig. 2B). This unambiguously proved a disease burden-dependent correlation between BM-MRD and PB-MRD. In addition to disease status, we focused on BM infiltration at sampling and collection time point for the subgroup analysis according to each sample evaluation. As naturally expected, BM infiltration at sampling had a strong impact on the correlation between BM-MRD and PB-MRD and separated 133 sample pairs into the strongly correlated-positive subgroup of 21 sample pairs (r = 0.736) and the weakly correlated-negative subgroup of 112 sample pairs (r = 0.306) (Fig. 2A). It is noteworthy to point out that even the BM infiltration-negative subgroup has a weak correlation, confirming a superior sensitivity of ddPCR to conventional pathological method in detecting BM-MRD. In terms of collection time point, we found a strong correlation in the relapse subgroup as expected from active disease progression. The observed moderate correlation in the treatment subgroup may reflect the disassemble of tumor (in primary site and BM) and the subsequent release of tumor cells into PB (Fig. 2C). This speculation is supported by the two facts: 1) Tumor (in primary site and BM) and MRD (in PB and BM) are decreased in response to treatment. 2) The relative abundance of BM-MRD and PB-MRD is changed from the BM-dominant at diagnosis (BM median 2896.3 vs. PB median 39.4, Fig. 2C) to the PB-main during treatment (PB median 5.6 vs. BM median 3.3, Fig. 2C). To our surprise, the correlation in the diagnosis subgroup did not reach a

statistical significance. It may be due to a large variation in the timing of initial diagnosis compared to relapse diagnosis, as the first diagnosis of NB was made only when a patient came in the hospital.

Analyses of subgroups according to each patient evaluation also provided complementary results of the present study. Established NB prognostic factors [35, 44, 45]of age at diagnosis, BM metastasis at diagnosis, and DNA ploidy were found to separate 133 pairs into the moderately correlated ($r = 0.418–0.478$)-poor prognosis subgroups (93–122 sample pairs) and the uncorrelated-good prognosis subgroups (11–33 sample pairs) (Fig. 3). These findings were consistent with and strengthened a disease burden-dependent correlation between BM-MRD and PB-MRD. However, there were limitations in the present study; small number of patients and samples (19 patients and 133 samples), no significant correlation in the diagnosis subgroup (Fig. 2), and little difference between MYCN-amplified and non-amplified subgroups (Supplementary Figure 1). Further studies with larger number of samples and patients will be required to confirm the present results.

The dynamic and disease burden-dependent correlation between BM-MRD and PB-MRD in high-risk NB patients is reminiscent of the molecular response-dependent correlation of BCR-ABL mRNA expression between BM and PB in tyrosine kinase inhibitor-treated CML patients [20]. Like hematologic malignancies of CML, NB cells detected in PB may originate from NB cells resided in BM. Although SAPs have been believed to be the cellular origin of NB, the majority of normal adrenal chromaffin cells are recently shown to be derived from SCPs in mouse genetic models [1]. Furthermore, mouse hematopoietic and mesenchymal stem cells have shown to be derived from SCP-containing NC derivatives [24–27]. Given that NB predominantly developed at adrenal gland and most frequently metastasized and relapsed in BM, the NC-derived SCPs may develop NB at adrenal gland and migrate into BM in human NB patients. Therefore, present study will provide a clinical support for the mouse observations [3, 24–27] and may explain why BM is the most frequent site of metastasis and relapse in non-hematopoietic solid tumor of NB [28].

In conclusion, we have revealed that MRD in high-risk NB shows a dynamic and disease burden-dependent correlation between BM and PB by using an extended cohort of NB patients and samples.

Declaration of Competing Interest

N.Nis received an institutional research funding from Sysmex Corporation to Kobe University. The other authors have no competing interests to declare.

Acknowledgements

We thank all staffs of Pediatric department at Kobe University Hospital and Hematology and Oncology department at Kobe Children's Hospital for collecting BM and PB samples.

Funding

The present study was supported in part by Grants-in-Aid for Scientific Research (KAKENHI) from Japan Society for the Promotion of Science (No.17K10110, No.19K17361, and No.19K17331) and an institutional research funding from Sysmex Corporation to Kobe University (N.Nis.).

Author Contributions

Kyaw San Lin: Conceptualization, Formal analysis, Investigation, Visualization, Writing - Original Draft, Writing - Review & Editing. Suguru Uemura: Formal analysis, Investigation, Visualization, Writing - Review & Editing. Khin Kyae Mon Thwin: Formal analysis, Investigation, Visualization, Writing - Review & Editing. Naoko Nakatani: Formal analysis, Investigation. Toshiaki Ishida: Conceptualization, Formal analysis, Investigation, Writing - Review & Editing. Nobuyuki Yamamoto: Conceptualization, Formal analysis, Investigation, Writing - Review & Editing. Akihiro Tamura: Formal analysis, Investigation. Atsuro Saito: Formal analysis, Investigation. Takeshi Mori: Formal analysis, Investigation. Daiichiro Hasegawa: Conceptualization, Supervision, Writing - Review & Editing. Yoshiyuki Kosaka: Conceptualization, Supervision, Writing - Review & Editing. Nanako Nino: Formal analysis, Investigation. China Nagano: Formal analysis, Investigation. Satoru Takafuji: Formal analysis, Investigation. Kazumoto Iijima: Conceptualization, Supervision, Writing - Review & Editing. Noriyuki Nishimura: Conceptualization, Data curation, Funding acquisition, Project administration, Resources, Supervision, Writing - Original Draft, Writing - Review & Editing.

Supplementary materials

Supplementary material associated with this article can be found, in the online version, at doi:10.1016/j.tranon.2021.101019.

References

[1] A. Furlan, V. Dyachuk, M.E. Kastriti, et al., Multipotent peripheral glial cells generate neuroendocrine cells of the adrenal medulla, Science 357 (2017) eaal3753.
[2] S. Tsubota, K. Kadomatsu, Origin and initiation mechanisms of neuroblastoma, Cell Tissue Res 372 (2018) 211–221.
[3] C. Delloye-Bourgeois, V. Castellani, Hijacking of embryonic programs by neural crest-derived neuroblastoma: from physiological migration to metastatic dissemination, Front Mol Neurosci 12 (2019) 52.
[4] G.M. Brodeur, Neuroblastoma: biological insights into a clinical enigma, Nat Rev Cancer 3 (2003) 203–216.
[5] J.M. Maris, M.D. Hogarty, R. Bagatell, S.L. Cohn, Neuroblastoma, Lancet 369 (2007) 2106–2120.
[6] V.P. Tolbert, K.K. Matthay, Neuroblastoma: clinical and biological approach to risk stratification and treatment, Cell Tissue Res 372 (2018) 195–209.
[7] K. Beiske, P.F. Ambros, S.A. Burchill, I.Y. Cheung, K. Swerts, Detecting minimal residual disease in neuroblastoma patients-the present state of the art, Cancer Lett 228 (2005) 229–240.
[8] S.C. Brownhill, S.A. Burchill, PCR-based amplification of circulating RNAs as prognostic and predictive biomarkers - Focus on neuroblastoma, Pract Lab Med 7 (2017) 41–44.
[9] J. Stutterheim, L. Zappeij-Kannegieter, R. Versteeg, H.N. Caron, C.E. van der Schoot, G.A.M. Tytgat, The prognostic value of fast molecular response of marrow disease in patients aged over 1 year with stage 4 neuroblastoma, Eur J Cancer 47 (2011) 1193–1202.
[10] V.F. Viprey, W.M. Gregory, M.V. Corrias, et al., Neuroblastoma mRNAs predict outcome in children with stage 4 neuroblastoma: a European HR-NBL1/SIOPEN study, J Clin Oncol 32 (2014) 1074–1083.
[11] N.K. Cheung, I. Ostrovnaya, D. Kuk, I.Y. Cheung, Bone marrow minimal residual disease was an early response marker and a consistent independent predictor of survival after anti-GD2 immunotherapy, J Clin Oncol 33 (2015) 755–763.
[12] A. Marachelian, J.G. Villablanca, C.W. Liu, et al., Expression of five neuroblastoma genes in bone marrow or blood of patients with relapsed/refractory neuroblastoma provides a new biomarker for disease and prognosis, Clin Cancer Res 23 (2017) 5374–5383.
[13] K.K.M. Thwin, T. Ishida, S. Uemura, et al., Level of seven neuroblastoma-associated mRNAs detected by droplet digital pcr is associated with tumor relapse/regrowth of high-risk neuroblastoma patients, J Mol Diagn 22 (2020) 236–246.
[14] S.A. Burchill, P.J. Selby, Molecular detection of low-level disease in patients with cancer, J Pathol 190 (2000) 6–14.
[15] P. Mordant, Y. Loriot, B. Lahon, et al., Minimal residual disease in solid neoplasia: new frontier or red-herring? Cancer Treat Rev 38 (2012) 101–110.
[16] S. Uemura, T. Ishida, K.K.M. Thwin, et al., Dynamics of minimal residual disease in neuroblastoma patients, Front Oncol 9 (2019) 455.
[17] H. Wang, N.H. Stoecklein, P.P. Lin, O. Gires, Circulating and disseminated tumor cells: diagnostic tools and therapeutic targets in motion, Oncotarget 8 (2017) 1884–1912.
[18] E. Coustan-Smith, J. Sancho, M.L. Hancock, et al., Use of peripheral blood instead of bone marrow to monitor residual disease in children with acute lymphoblastic leukemia, Blood 100 (2002) 2399–2402.
[19] K. Kitamura, T. Nishiyama, K. Ishiyama, et al., Clinical usefulness of WT1 mRNA expression in bone marrow detected by a new WT1 mRNA assay kit for monitoring acute myeloid leukemia: a comparison with expression of WT1 mRNA in peripheral blood, Int J Hematol 103 (2016) 53–62.
[20] Q. Jiang, X.Y. Zhao, Y.Z. Qin, et al., The differences and correlations of BCR-ABL transcripts between peripheral blood and bone marrow assays are associated with the molecular responses in the bone marrow for chronic myelogenous leukemia, Am J Hematol 87 (2012) 1065–1069.
[21] A. Stathopoulou, I. Vlachonikolis, D. Mavroudis, et al., Molecular detection of cytokeratin-19-positive cells in the peripheral blood of patients with operable breast cancer: evaluation of their prognostic significance, J Clin Oncol 20 (2002) 3404–3412.

[22] C. Shen, L. Hu, L. Xia, Y. Li, Quantitative real-time RT-PCR detection for survivin, CK20 and CEA in peripheral blood of colorectal cancer patients, Jpn J Clin Oncol 38 (2008) 770–776.
[23] L. Dardaei, R. Shahsavani, A. Ghavamzadeh, et al., The detection of disseminated tumor cells in bone marrow and peripheral blood of gastric cancer patients by multimarker (CEA, CK20, TFF1 and MUC2) quantitative real-time PCR, Clin Biochem 44 (2011) 325–330.
[24] J.Y. Bertrand, N.C. Chi, B. Santoso, S. Teng, D.Y. Stainier, D. Traver, Haematopoietic stem cells derive directly from aortic endothelium during development, Nature 464 (2010) 108–111.
[25] K. Kissa, P. Herbomel, Blood stem cells emerge from aortic endothelium by a novel type of cell transition, Nature 464 (2010) 112–115.
[26] J.C. Boisset, W. van Cappellen, C. Andrieu-Soler, N. Galjart, E. Dzierzak, C. Robin, In vivo imaging of haematopoietic cells emerging from the mouse aortic endothelium, Nature 464 (2010) 116–120.
[27] J. Isern, A. Garcia-Garcia, A.M. Martin, et al., The neural crest is a source of mesenchymal stem cells with specialized hematopoietic stem cell niche function, Elife 3 (2014) e03696.
[28] S.A. Burchill, K. Beiske, H. Shimada, et al., Recommendations for the standardization of bone marrow disease assessment and reporting in children with neuroblastoma on behalf of the International Neuroblastoma Response Criteria Bone Marrow Working Group, Cancer 123 (2017) 1095–1105.
[29] T.J. Moss, D.G. Sanders, Detection of neuroblastoma cells in blood, J Clin Oncol 8 (1990) 736–740.
[30] R.C. Seeger, C.P. Reynolds, R. Gallego, D.O. Stram, R.B. Gerbing, K.K. Matthay, Quantitative tumor cell content of bone marrow and blood as a predictor of outcome in stage IV neuroblastoma: a Children's Cancer Group Study, J Clin Oncol 18 (2000) 4067–4076.
[31] Y. Yanez, D. Hervas, E. Grau, et al., TH and DCX mRNAs in peripheral blood and bone marrow predict outcome in metastatic neuroblastoma patients, J Cancer Res Clin Oncol 142 (2016) 573–580.
[32] J. Stutterheim, A. Gerritsen, L. Zappeij-Kannegieter, et al., Detecting minimal residual disease in neuroblastoma: the superiority of a panel of real-time quantitative PCR markers, Clin Chem 55 (2009) 1316–1326.
[33] N. Yamamoto, A. Kozaki, T.B. Hartomo, et al., Differential expression of minimal residual disease markers in peripheral blood and bone marrow samples from high--risk neuroblastoma patients, Oncol Lett 10 (2015) 3228–3232.
[34] J.L. Weinstein, H.M. Katzenstein, S.L. Cohn, Advances in the diagnosis and treatment of neuroblastoma, Oncologist 8 (2003) 278–292.
[35] S.L. Cohn, A.D.J. Pearson, W.B. London, et al., The International Neuroblastoma Risk Group (INRG) classification system: an inrg task force report, J Clin Oncol 27 (2009) 289–297.
[36] W.B. London, V. Castel, T. Monclair, et al., Clinical and biologic features predictive of survival after relapse of neuroblastoma: a report from the International Neuroblastoma Risk Group project, J Clin Oncol 29 (2011) 3286–3292.
[37] T. Hishiki, K. Matsumoto, M. Ohira, et al., Results of a phase II trial for high-risk neuroblastoma treatment protocol JN-H-07: a report from the Japan Childhood Cancer Group Neuroblastoma Committee (JNBSG), Int J Clin Oncol 23 (2018) 965–973.
[38] G.M. Brodeur, J. Pritchard, F. Berthold, et al., Revisions of the international criteria for neuroblastoma diagnosis, staging, and response to treatment, J Clin Oncol 11 (1993) 1466–1477.
[39] J.F. Huggett, C.A. Foy, V. Benes, et al., The digital MIQE guidelines: minimum information for publication of quantitative digital PCR experiments, Clin Chem 59 (2013) 892–902.
[40] P. Schober, C. Boer, L.A. Schwarte, Correlation coefficients, Anesth Analg 126 (2018) 1763–1768.
[41] A.K. Akobeng, Understanding diagnostic tests 3: receiver operating characteristic curves, Acta Paediatr 96 (2007) 644–647.
[42] Y. Kanda, Investigation of the freely available easy-to-use software 'EZR' for medical statistics, Bone Marrow Transplant 48 (2013) 452–458.
[43] T.B. Hartomo, A. Kozaki, D. Hasegawa, et al., Minimal residual disease monitoring in neuroblastoma patients based on the expression of a set of real-time RT-PCR markers in tumor-initiating cells, Oncol Rep 29 (2013) 1629–1636.
[44] K.T. Vo, K.K. Matthay, J. Neuhaus, et al., Clinical, biologic, and prognostic differences on the basis of primary tumor site in neuroblastoma: a report from the International neuroblastoma risk group project, J Clin Oncol 32 (2014) 3169–3176.
[45] D.A. Morgenstern, U. Potschger, L. Moreno, et al., Risk stratification of high-risk metastatic neuroblastoma: a report from the HR-NBL-1/SIOPEN study, Pediatr Blood Cancer 65 (2018) e27363.